Available online at www.sciencedirect.com
SCIENCE DIRECT®
Bioelectrochemistry 63 (2004) 217–224
Bioelectrochemistry
www.elsevier.com/locate/bioelechem

Application of integrated SECM ultra-micro-electrode and AFM force probe to biosensor surfaces

Yoshiki Hirata*, Soichi Yabuki, Fumio Mizutani

National Institute of Advanced Industrial Science and Technology (AIST), Central 6, Higashi 1-1-1 Tsukuba, Ibaraki, 305-8566, Japan

Received 23 June 2003; received in revised form 25 January 2004; accepted 27 January 2004

Abstract

The integration of scanning electrochemical ultra-micro-electrode (UME) with atomic force microscope cantilever probe have been achieved by using a homemade photolithography system. A gold-film-coated AFM cantilever was insulated with photo resist coating and a pointed end of the AFM probe was opened by illuminating with maskless arbitrary optical micro-pattern generator. To realize precise control of probe sample distance constantly, the resulting scanning electrochemical microscopy (SECM)–AFM probe was operated using a dynamic force microscopy (DFM) technique with magnetic field excitation. From a steady-state voltammetric experiment, the effective electrode diameters of the probes thus prepared were estimated to be from 0.050 to 6.2 μm. The capability of this SECM–AFM probe have been tested using gold comb in the presence of $Fe(CN)_6^{3-}$. The simultaneous imaging of the topography and electrochemical activity of the strip electrode was successfully obtained. We also used the SECM–AFM to examine in situ topography and enzymatic activity measurement. Comparison of topography and oxidation current profiles above enzyme-modified electrode showed active parts distribution of biosensor surface.

Keywords: Scanning electrocahemical microscopy; SECM; Atomic force microscopy; AFM; Enzyme-modified electrode; Biosensor

1. Introduction

Scanning electrochemical microscopy (SECM) is a powerful tool to study both for high-precision control of surface processes, such as nano-fabrication [1,2], and for high-resolution imaging of interfacial activity [3]. Recently, reviews on various aspects of SECM from theory to application have appeared [4–6]. In conventional SECM experiments, the ultra-micro-electrode (UME) tip is scanned in constant height above the sample surface. The faradic current measured at the UME is mainly influenced by the reactivity and morphology of the sample, the distance between tip and sample, and the size and geometry of the UME when the electrode is closed proximity. However, a weak point of the previous SECM system is the lack of spatial resolution compared with conventional scanning probe microscopes, such as AFM or STM, due to a current-dependent positioning of the micro-electrode. The introduction of the probe controlling system for AFM, which shows much higher spatial resolution, to the SECM is a particularly attractive for an electrochemical–topographical imaging with enhanced spatial resolution. Several approaches have been reported for combination of the SECM probe and an alternative tip positioning strategy during SECM experiments.

Recent developments focused on the combination of AFM and SECM enable positioning of the UME independently of the current response during simultaneous high resolution. The first approach of dual functioning probe was fabricated by coating a flattened and etched Pt micro wire with an insulator. The flattened part of the probe acts as a flexible cantilever while the coating insulates the probe such that only the tip end is exposed to the solution [7,8]. Although high spatial resolution was achieved, imaging with this type of dual functioning probe in contact mode is limited to its applications. Alternatively, a dual functioning probe on can be fabricated by focused ion beam (FIB) milling of metal-coated cantilever tips creating an electroactive area at a preselected region above the probe [9,10].

* Corresponding author. Tel.: +81-29-861-9433; fax: +81-29-861-6177.
E-mail address: y-hirata@aist.go.jp (Y. Hirata).

1567-5394/$ - see front matter © 2004 Elsevier B.V. All rights reserved.
doi:10.1016/j.bioelechem.2004.01.001

However, these techniques require a high cost and time is rather troublesome. An alternative method is combining SECM probe with near-field scanning optical microscopy (NSOM) optical fiber probe. In NSOM, mechanically actuated shear force based positioning of optical fibers with the use of optical detection techniques [11] or non-optical detection based on tuning fork resonator system [12] have been used. Surface shear force increases because of hydrodynamic effects in close proximately to the sample and leads to amplitude damping and phase shift of the oscillation [13]. In these case, NSOM system can be converted to SECM by replacement of optical fiber to various kinds of UME [14,15]. However, there are still some difficulty in reproducing of nanometer size UME fabricated by conventional techniques such as fiber puller [16].

In this work, we have proposed the integration of an UME in an AFM force probe by using a simple photolithographic techniques. A gold-film-coated AFM cantilever was insulated with photo resist coating. Then a pointed end of the AFM probe was opened by illuminating with an optical micro-pattern generator without the use of a mask. To realize precise control of probe sample distance constantly, resulting SECM–AFM probe was tried to operate using dynamic force microscopy (DFM) technique with magnetic field excitation. This paper described preliminary results for the measurement of redox reaction over gold strip test electrodes and for the measurements of glucose oxidase (GOD) biosensor surface.

2. Experiments

2.1. Preparation of SECM–AFM probe

Fig. 1(a) shows the preparation procedure for the SECM–AFM probes. An oxide sharpened silicon nitride AFM probe (DNPS, Veeco Instruments). Short narrow triangular lever (120 μm long) was used. The nominal spring constant is 0.12 N/m. Before the preparation procedure, cantilevers were carefully cleaned as follow. The cantilever purchased was cleaned by incubating for 30 min in acetone, washed with milli-Q water and dried in N_2 gas flow. Then the cantilever was cleaned by UV light irradiation. During this process, remaining organic contaminants on the cantilever surface were oxidized by photochemical oxidation reaction [17,18]. The conductive coating was formed by vacuum deposition of chromium and gold film (thickness: ca. 0.1–0.2 nm, 30–100 nm, respectively) under high vacuum (below 5×10^{-5} Pa). The film thickness and deposition rate were monitored using quartz crystal microbalance (XTM/2, Leybold Inficon). To prepare smooth gold surface deposition rate was kept at 0.01–0.03 nm s^{-1}. The calibration was performed measuring the thickness of deposited test strip height using AFM. Successively insulating coating of photo resist layer (SPP, NTT-AT) was formed on gold layer by touching soft sponge containing an ethanol-diluted photo resist solution (1:2 by volume). The thickness of insulating layer was controlled dilution ratio of photo resist. The coated lever was beaked at 110 °C on the hotplate. To avoid the pinhole formation around the tip apex, cantilevers were placed with tip side down. The probe opening and connecting part were formed by using light illumination by using homemade simple photo lithography system. Schematic of was illustrated in Fig. 1(b). This system consists of an upright optical microscope (BX50, Olympus and M plan NUV100 objective lens, Mitutoyo) with illumination port and DMD (Digital Micro-mirror Device) type PC video projector (TH-100LG1, Panasonic). A small circle was drawn using presentation software (Power Point98™, Microsoft), then the image was projected on the apex of photo resist coated AFM cantilever through the illumination port of the optical microscope. The irradiated part was removed by developing, using alkaline solution (NMD-W, Tokyo Ohka Kogyo), and then washing with milli-Q water gently.

2.2. Dynamic force microscopy operation of SECM–AFM in aqueous solutions

All experiments were performed using a Digital Instruments Nanoscope™ IIIa with a Bioscope™ scanning head. A SECM–AFM probe was mounted on the glass liquid cell. For the electronic connection between probe and outer circuit, a kapton sandwiched flexible copper thin film (a gift from Ube Industry) was glued using silver past (RS components). The liquid contact regions were carefully sealed using epoxy resin. To oscillate the SECM–AFM probe in the liquid solutions, a small ferromagnetic bead (10–30 μm in diameter, TB3030, Toda Industry) was glued behind the cantilever by using two armed micro manipulator. The bead attached probe was actuated by a solenoid coil (ca. 25 mm ∅, 150 turns, 0.2 mm ∅ enamel-coated copper wire) placed in the neighborhood. In a DFM operation, the cantilever oscillation was monitored instead of the deflection since change of oscillation frequency was monitored and maintained constant using phase-locked loop (PLL) electronics (KH-2001, Kyoto Instruments). The lever oscillation amplitude, phase shift and resonant frequency were changed due to the tip–sample interaction.

2.3. Preparation of enzyme electrode

The enzyme used was GOD (EC 1.1.3.4, from *Aspergillus* sp., Grade II, Toyobo). Poly-L-lysine hydrobromide (molecular weight, 90,000) was obtained from sigma chemicals. Poly(sodium 4-styrenesulfonate) (molecular weight, 70,000) was purchased from Aldrich. Polystylene sulfonate solution (20 μl; 25 μM as monomer unit), GOD solution (20 μM; 2 wt.%) and poly-L-lysine solution (20 μl; 25 μM as monomer unit) were successively dropped on the surface of freshly cleaved HOPG

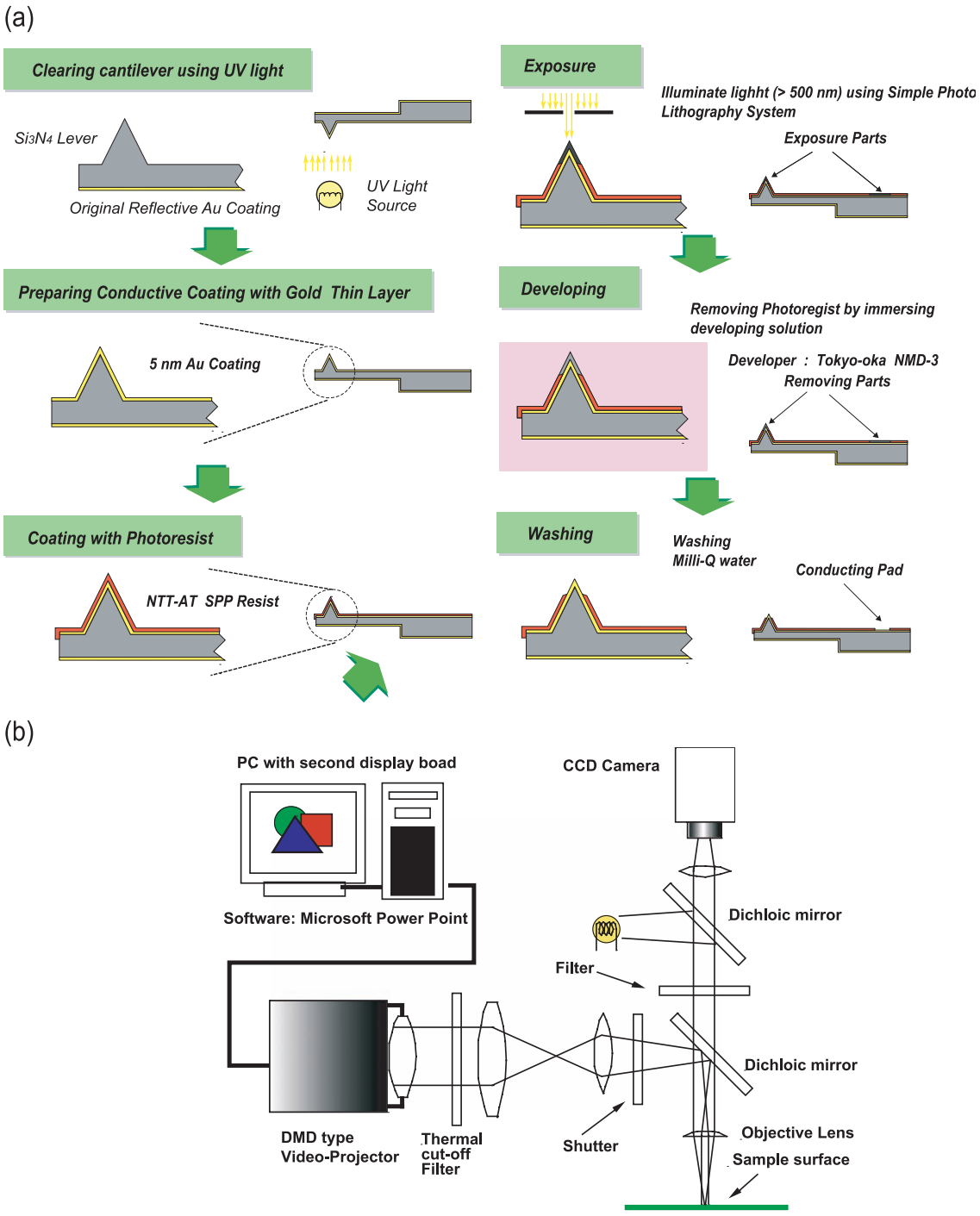

Fig. 1. (a) Schematic illustration of preparation procedure of SECM–AFM probe. (b) Schematic diagram of the maskless arbitrary optical micro-pattern generator. The virtual mask image illustrated on the CRT is projected by DMD-type video projector through the illumination port of optical microscope.

surface, and then dried under decompression condition for 4 h.

2.4. Electrochemical measurements

Both sample and probe potentials were controlled by using a multi channel potentiostat (HA1010mM2S-S, Hokuto Denko). A saturated calomel electrode (SCE) and a Pt wire were used for the reference and counter electrode, respectively. All solutions were prepared by using Milli-Q water (Millipore) regent water. For a standard sample of SECM, a gold interdigitated array electrode (IDA) (10 μm width, 4 μm gap, 200 nm finger height; NTT-AT) on glass substrate was used.

3. Results and discussion

3.1. Electrochemistry of cantilever micro-electrode

The exposed area of SECM–AFM probe was determined by steady-state voltammetry experiments. The SECM current and potential characteristics on a given probe were found to be reproducible and stable for a few weeks in 10 mM $K_3[Fe(CN)_6]$ and 0.1 M KCl at a scan rate of 50 mV/s. A reduction oxidation cleaning process was effective to clean the small aperture, but applying too much potential had caused serious damage of the probe. The safety potential region was -0.6 to $+1.3$ V vs. SCE. By measuring a diffusion-controlled current, we can estimate the probe opening by assuming that the exposed tip is hemispherical [7].

$$i_{(\infty)} = 2\pi naFDC \quad (1)$$

where D and C are the diffusion coefficient and concentration of the electroactive species, n is the number of transferred electron for the redox reaction, F is Faraday constant and a is the radius of the electrode. By changing illumination area, we could control aperture diameter from 0.050 to 6.2 μm. The influence of probe oscillation on the shape of voltammogram was examined in the same condition of steady experiment except the oscillation of probe. The voltammogram obtained under the oscillation was almost same shape and the capacitance but current was slightly large. Compared with the thickness of diffusion layer, the probe oscillation amplitude of ~ 2 nm can be negligible.

3.2. Dynamic force microscopy operation of SECM–AFM in aqueous solutions

DFM which utilizes the resonance enhancement of the force sensitivity by oscillating the cantilever at resonance frequency provides us a powerful operating mode for atomic force microscopy [19]. In the DFM mode, the high mechanical Q-factor of the cantilever is utilized to increase force sensitivity. In a liquid environment, the mechanical Q-factor of the cantilever is drastically reduced due to the viscosity of the liquid. Recently, some groups have examined to achieve high force sensitivity as follows. Jarvis et al. [20] mounted a tiny magnetized particles on the cantilever to utilize a frequency modulation (FM) detection method by exciting the cantilever with magnetic force. Fuchs et al. [21] also presented high force sensitivity utilizing the phase detection method enhanced by using the Q-control electronics. Tamayo et al. [22] extended the amplitude detection method with the Q-control electronics. In this paper, we show the FM detection can be used in a liquid environment by exciting the SECM–AFM probe by the magnetic field.

Before DFM mode experiments in liquid environment, we measured resonance characteristics of the cantilever. The spectra were measured by using a waveform synthesizer HP33120A (Hewlett Packard) in frequency sweep mode. Fig. 2(a) shows free oscillation spectra of the SECM–AFM probe while the cantilever is mechanically actuated in the ambient. The broken line in Fig. 2(a) shows oscillation spectrum of cantilever without any modification (not exactly same lever but in same lots). A comparison of spectrum with and without modification, the cantilever modification process during SECM–AFM fabrication, the resonance frequency change of cantilever was not more than 1.5 kHz in the ambient. Also, the Q-factor was slightly affected by this

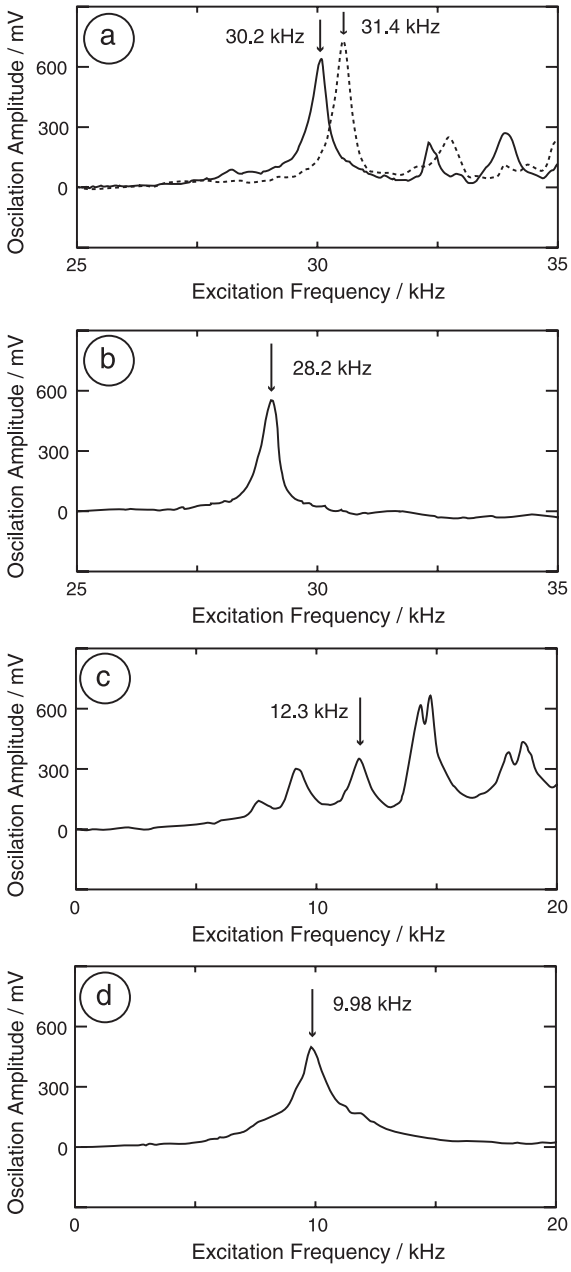

Fig. 2. The resonance spectra of the SECM–AFM cantilever probe (a, c) in ambient and (b, d) in liquid environment. Resonance peaks of cantilevers are indicated by arrow. The probe was actuated by (a, b) mechanically and by (c, d) magnetic field. The natural resonance spectrum of unmodified AFM cantilever was shown in (a) by broken line.

modification. Fig. 2(c) is free oscillation spectrum of the cantilever while the cantilever is mechanically actuated, obtained in a liquid (milli-Q water). In this case, many higher-order resonance peaks were observed caused by the complex mechanical interaction between the piezo actuator and the cantilever through the liquid. The measured free resonance frequency in the ambient was 28.2 kHz and the *Q*-factor was about 60. On the other hand, the resonance frequency went down around 12 kHz in liquid environment, which was about one-third of the free resonance in the ambient, and the *Q*-factor in water was as low as 2. In this situation, it is not easy to find out real resonance peak among artifact resonance peaks.

The spectra shown in Fig. 2(b) and (d) are measured in ambient and in liquid, respectively, while the magnetic field was applied. The resonance frequency was decreased about 2 kHz by attachment of magnetic bead. The artifact peaks were almost suppressed in magnetic excitation experiment. This simple nature of resonance peak in magnetic excitation gives us several advantages over mechanical one.

Fig. 3(a) shows the frequency shift curve plotted as a function of the probe-sample separation. The frequency shift in the vertical axis indicates the reduction of the resonance frequency from the value measured when the probe is far from the sample surface. The zero position of the gap distance is defined at the point where the oscillation amplitude was reached almost zero. The slope in the vicinity of the surface is steep enough to control the distance constantly by feed back electronics. By using this setup, the relationship between the current response on the tip for the reduction of the 5 mM $Fe(CN)_6^{3-}$ (at 0.6 V vs. SCE) and the distance between the tip and an insulating substrate as shown in Fig. 3(b). Due to the special sheltering of the diffusion volume, the magnitude of the reduction current decreased in associate with the decreased of the distance. Even at the glass surface, the reduction current do not go zero. This may reflect that the shape of the top end of SECM–AFM probe is a corn instead of a flat disk.

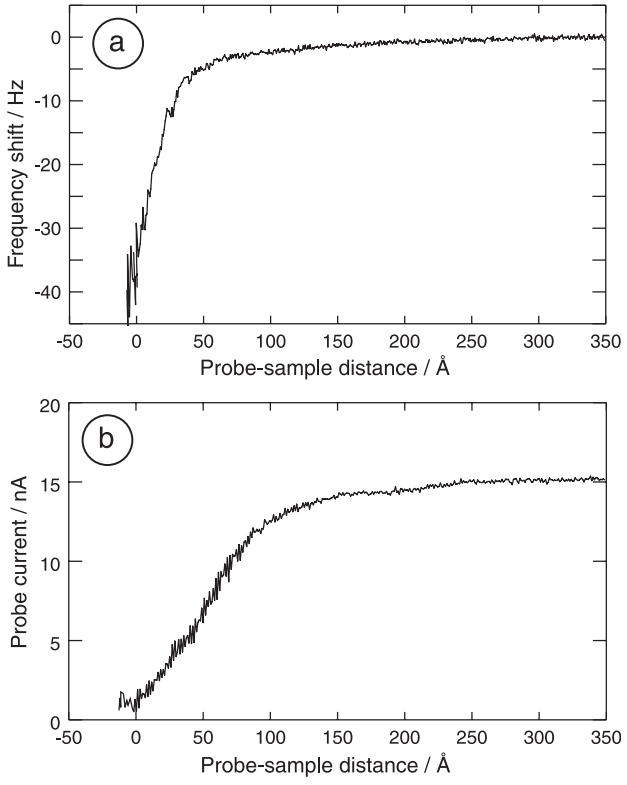

Fig. 3. Simultaneously recorded (a) frequency shift curve plotted as a function of the probe-sample separation and (b) Faraday current response curve for reduction of the 5 mM $Fe(CN)_6^{3-}$ (at 0.6 V vs. SCE).

3.3. Performance of SECM–AFM

In these conducting sample experiments, "non-contact" feature of the DFM mode becomes important. Accidental short circuit causes not only experimental error but also serious damage of sample and probe. To avoid direct contact, we set the oscillation amplitude not more than 2 nm peak to peak and scanning rate of 0.8 Hz.

To clarify the characteristics of the SECM–AFM probe, we employed two kinds of experimental set up: One is the sample generation/probe correction mode and the other is the probe generation/sample correction mode. In the former case, the potential of the one side of IDA comb electrode was set at -0.1 V vs. SCE in order to proceed the reduction reaction of $Fe(CN)_6^{3-}$ to $Fe(CN)_6^{4-}$ and the other side of IDA comb electrode was set at $+0.6$ V to reoxidize $Fe(CN)_6^{4-}$: The reoxidation could avoid the accumulation of $Fe(CN)_6^{4-}$ near the electrode surface. The probe potential was set at 0.6 V and probe current was measured. The test solution contains 5 mM of $Fe(CN)_6^{4-}$, 5 mM of $Fe(CN)_6^{3-}$ and 50 mM KCl. Fig. 4 shows (a) topographic image and (b) probe current image over gold IDA electrode surface. The anodic probe current was observed on the IDA comb whose potential was set at 0 V, but such a current was not obtained on the glass surface. Since the reaction is diffusion controlled at this potential, the probe current was in proportional to the $Fe(CN)_6^{4-}$ concentration. Above the IDA comb with a potential of $+0.6$ V, the probe current was lower than glass surface. In the current image, there are no spike noises attributed from direct contact between probe and sample, and the distance control of DFM in liquid environment is satisfactory.

The next set up is the probe generation sample correction mode. In this case, the IDA electrode was the same controlled potential (two IDA electrodes were connected and controlled 0.6 V) and probe current was measured. The test solution contains 5 mM of $Fe(CN)_6^{3-}$ and 50 mM KCl. The concurrently recorded (c) topography and (d) current image over IDA electrode surface are shown. The probe releases the reduced species (the potential of probe, -0.2 V vs. SCE), which diffuses to the electroactive site of the IDA comb electrode then oxidized. In the current image, the anodic probe current was set to positive for reason of

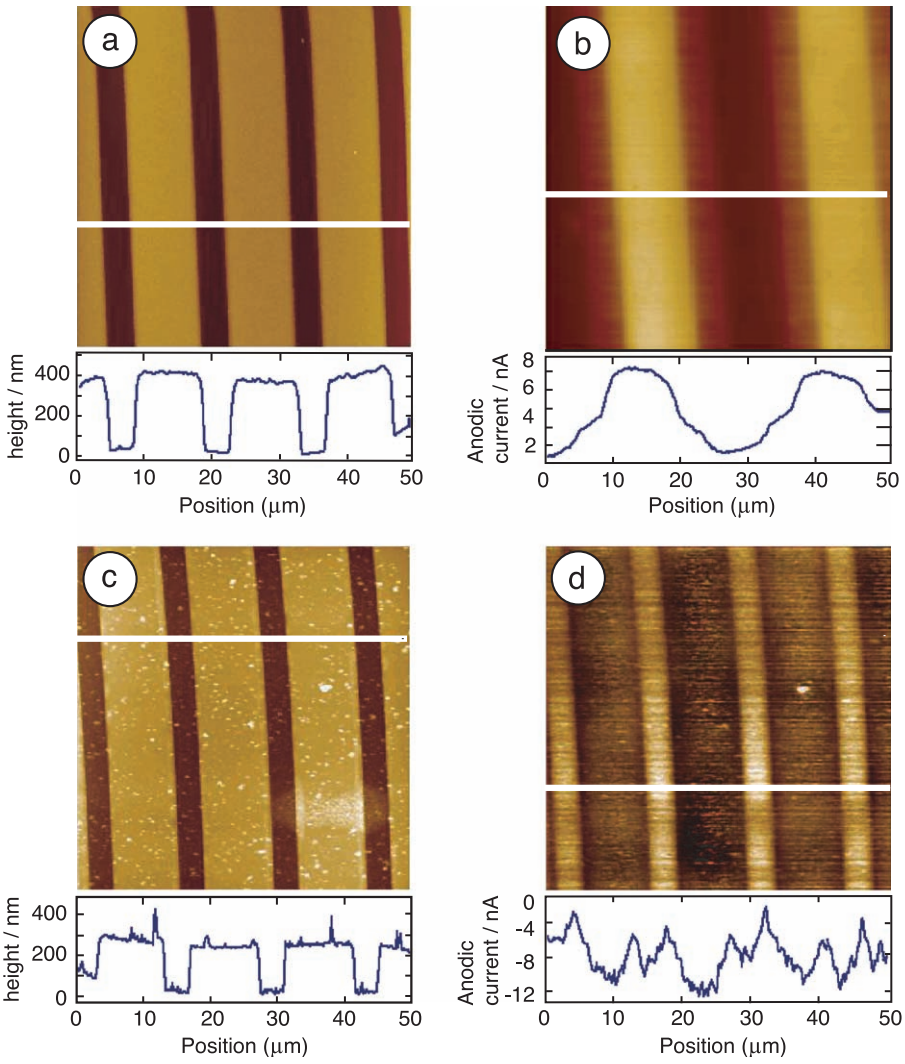

Fig. 4. Simultaneously recorded topographic images and SECM current images of gold IDA electrodes obtained from the sample generation/probe correction mode (a, c) and the probe generation/sample correction mode (b, d) together with cross sections. In the sample generation/probe correction mode, the probe was polarized at +0.6 V vs. SCE, and the anodic probe current was measured (b). One of the IDA electrodes was polarized at −0.1 V and the other was set to +0.6 V. In the probe generation/sample correction mode, the probe potential was set at −0.2 V, and the anodic probe current was recorded. The IDA combined electrodes were connected and set at +0.6 V.

polarity of A/D converter. The oxidation results increasing in the sample current and oxidized species diffuse back to the probe where it increased the concentration of electroactive species. Using this technique, spatial resolution of SECM current image is much improved in this set up, however, the noise level in the current signal increased. Further improvement of the resolution could be achieved by optimizing the experimental parameter such as spring constant of the cantilever, resonance frequency, oscillation amplitude and so on.

3.4. Imaging of enzyme-modified electrode surface

Enzyme-based amperometric biosensor have attracted interest because high sensitivity and selectivity. Recently, we have found that enzymes could be immobilized into a poly-ion complex membrane prepared from poly-L-lysine and poly(4-styrenesulfonate) and that the membrane showed permoselectivity based on the solute size with the molecular cut-off of 110. Enzyme molecules could be entrapped into the ionically cross-linked complex, and the cross-linked topology is useful for the selective permeation of small molecule solute [23–25]. Fig. 5(a) shows topographic image of a poly ion complex layer containing glucose-oxidase-modified graphite (HOPG) electrode surface. Many small grains were observed in relatively thin and smooth layer. Only from this topographic image could we not identify these aggregates. Fig. 5(b) and (c) shows SECM current images of before and after addition of glucose solution, respectively. These images were taken in air-saturated 10 mM phosphate buffer (pH 7.4). The probe potential was set to +0.9 V, which

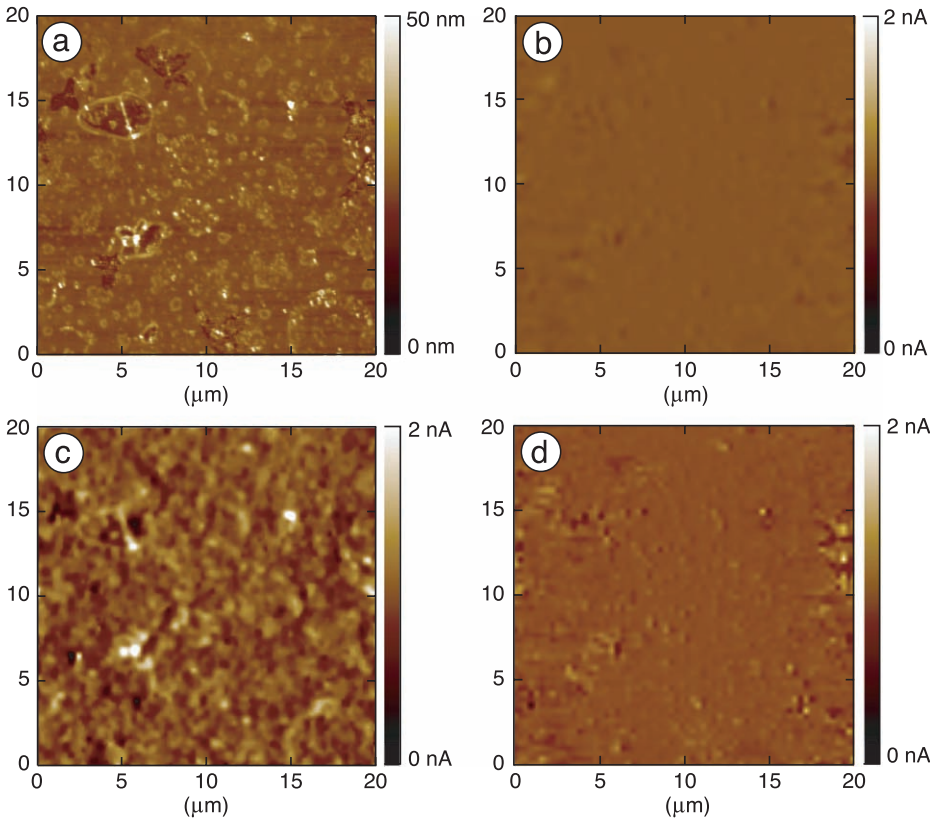

Fig. 5. Simultaneously recorded topography and SECM current images of a polyion complex layer containing glucose-oxidase-modified graphite (HOPG) electrode using DFM mode SECM–AFM. The probe was oscillated at 10.7 kHz and imaging frequency shift was set at −20 Hz. The probe current was monitored. (a) Topographic image; (b) SECM current image (probe potential: +0.9 V) taken without glucose; (c) SECM current image taken at 10 mM glucose; (d) same condition as (c) but base electrode potential was set to +0.9 V.

was high enough for the oxidation reaction of H_2O_2 proceeds. In these experiments, the base HOPG electrode was electrically floated, which only acts as a supported substrate. In the absence of glucose, the current recorded at the SECM–AFM probe is almost negligible as shown in Fig. 5(b). In the presence of glucose (ca. 10 mM), an increase of oxidation current of H_2O_2 was monitored (Fig. 5(c)). The addition of glucose solution resulted on a remarkable increase of oxidation current mainly at the aggregation part. The resolution of current image is so high that we can recognized a grain, an aggregation and a membrane defect in comparison to topography. However, quantitative analysis of this membrane was difficult from this preliminary result.

On this type of enzyme-modified electrode, oxidase was used for immobilization and hydrogen peroxide was detected on the base electrode:

$$\text{Substrate} + O_2 \rightarrow \text{Product} + H_2O_2 \quad (2)$$

For high sensitive detection, dissolved oxygen and substrate have to reach at the active enzyme site, and also the hydrogen peroxide which generated enzyme site as a result of reaction (2) has to arrive at base electrode surface. The increase of oxidation current signal may reflect the distribution of active enzyme spots or existence of effective passages of reactants and products. Fig. 5(d) shows SECM current image when the potential of base HOPG electrode was set to +0.9 V. In this condition, the H_2O_2 generated through the enzymatic reaction was consumed on the base electrode surface, so as to reduce current on the probe. From these data, comparison of topography and oxidation current profiles above GOD-modified electrode showed active parts distribution of biosensor surface. Wittstock et al. [2,26–28] have examined the use of conventional SECM in the modification and characterization of enzyme-modified patterned monolayers, enzyme-modified polymer microstructures and enzyme-modified metal microstructures. Such structural configurations are important for the development of miniaturized bioanalytical systems, such as miniaturized enzyme electrode arrays. SECM has emerged as an ideal tool for evaluating such systems. More detailed understanding and devising of enzyme-modified electrodes, their methodology was highly suggestive. Further improvements of local current distribution could be achieved by optimizing the experimental setups.

In conclusion, we have successfully demonstrated the integration of scanning electrochemical UME with atomic force microscope cantilever probe by using a homemade photolithography system. The introduction of DFM positioning technique to SECM imaging was quite effective for

stable operation and high-precision imaging both current and topography. We found that these techniques could be applied not only to insulating surface but also to conducting electrode surface by working without direct contact. Examples include simultaneous recorded topographic and electrochemical images of IDA electrode and glucose-oxidase-modified electrode. The resolutions of both current and topography were high enough to visualize an activity of biomolecules. There is considerable prospect for applying this technique to probe a wide variety of biological processes and to examine the performance of micro devices, and so on.

References

[1] J.V. Macpherson, P.R. Unwin, A.C. Hillier, A.J. Bard, In-situ imaging of ionic crystal dissolution using an integrated electrochemical/AFM probe, J. Am. Chem. Soc. 118 (1996) 6445–6452.
[2] G. Wittstock, R. Hesse, W. Schuhmann, Patterned self-assembled alkanthiolate monolyers on gold. Patterning and imaging by means of scanning electrochemical microscopy, Electroanalysis 9 (1997) 746–750.
[3] F.F. Fan, A.J. Bard, Imaging of biological macromolecules on mica in humid air by scanning electrochemical microscopy, Proc. Natl. Acad. Sci. U. S. A. 96 (1999) 14222–14227.
[4] M.V. Mirkin, B.R. Horrocks, Electroanalytical measurements using the scanning electrochemical microscope, Anal. Chim. Acta 406 (2000) 119–146.
[5] C.E. Gardner, J.V. Macpherson, Atomic force microscopy probes go electrochemical, Anal. Chem., (2002) 576A–584A.
[6] G. Wittstock, Modification and characterization of artificially patterned enzymatically active surfaces by scanning electrochemical microscopy, Fresenius' J. Anal. Chem. 370 (2001) 303–315.
[7] J.V. Macpherson, P.R. Unwin, Combined scanning electrochemical–atomic force microscopy, Anal. Chem. 72 (2000) 276–285.
[8] J.V. Macpherson, P.R. Unwin, Noncontact electrochemical imaging with combined scanning electrochemical atomic force microscopy, Anal. Chem. 73 (2001) 550–557.
[9] C. Kranz, G. Friedbacher, B. Mizaikoff, A. Lugstein, J. Smoliner, E. Bertagnolli, Integrating an ultramicroelectrode in an AFM cantilever: combined technology for enhanced information, Anal. Chem. 73 (2001) 2491–2500.
[10] C. Lehrer, L. Frey, S. Petersen, Th. Sulzbach, O. Ohlsson, Th. Dziomba, H.U. Danzebrink, H. Ryssel, Fabrication of silicon aperture probes for scanning nearfield optical microscopy by focused ion beam nano machining, Microelectron. Eng. 721–728.
[11] E. Betzig, P.L. Finn, J.S. Weiner, Combined shear force and near-field scanning optical microscopy, Appl. Phys. Lett. 60 (1992) 2484–2486.
[12] R. Brunner, O. Hering, O. Marti, O. Hollricher, Piezoelectrical shear-force control on soft biological samples in aqueous solution, Appl. Phys. Lett. 71 (1997) 3628–3630.
[13] F.L. Toledo-Crow, P.C. Yang, Y. Chen, M. Vaez-Iravania, Near-field differential scanning optical microscope with atomic force regulation, Appl. Phys. Lett. 60 (1992) 2959–2967.
[14] M. Büchler, S.C. Kelley, W.H. Smyrl, Electrochem. Solid-State Lett. 3 (2000) 35–38.
[15] Y. Lee, Z. Ding, A.J. Bard, Combined scanning electrochemical/optical microscopy with shear force and current feedback, Anal. Chem. 74 (2002) 3634–3643.
[16] Y. Shao, M.V. Mirkin, G. Fish, S. Kokotov, D. Palanker, A. Lewis, Nanometersized electrochemical sensors, Anal. Chem. 69 (1997) 1627–1634.
[17] D.E. King, Oxidation of gold by ultraviolet light and ozone at 25 °C, J. Vac. Sci. Technol. A13 (1995) 1247–1253.
[18] H. Nonaka, A. Kurokawa, S. Ichimura, D.W. Moon, Ozone cleaning of carbon-related contaminants on Si wafers and other substrate materials, Mater. Res. Soc. Proc. 477 (1997) 493–498.
[19] K. Kobayashi, H. Yamada, H. Itoh, T. Horiuchi, K. Matsushige, Analog frequency modulation detector for dynamic force microscopy, Rev. Sci. Instrum. 72 (2001) 4383–4387.
[20] S.P. Jarvis, T. Ishida, T. Uchihashi, Y. Nakayama, H. Tokumoto, Frequency modulation detection atomic force microscopy in the liquid environment, Appl. Phys., A 72 (2001) S129–S132.
[21] B. Anczykowski, J.P. Cleveland, D. Krüger, V. Elings, H. Fuchs, Analysis of the interaction mechanisms in dynamic mode SFM by means of experimental data and computer simulation, Appl. Phys., A 66 (1998) S885–S889.
[22] J. Tamayo, A.D.L. Humphris, M.J. Miles, Piconewton regime dynamic force microscopy in liquid, Appl. Phys. Lett. 77 (2000) 582–584.
[23] F. Mizutani, S. Yabuki, Y. Hirata, Amperometric biosensors using poly-L-Lysine/poly-(stylenesulfonate) membranes with immobilized membrane, Denki Kagaku 63 (1995) 1100–1105.
[24] F. Mizutani, Y. Sato, Y. Hirata, T. Sawaguchi, S. Yabuki, Glucose oxidase/polyion complex-bilayer membrane for elimination of electroactive interferents in amperometric glucose sensor, Anal. Chim. Acta 364 (1998) 173–179.
[25] S. Yabuki, F. Mizutani, Y. Hirata, Hydrogen peroxide determination based on a glassy carbon electrode covered with polyion complex membrane containing peroxidase and mediators, Sens. Actuators B65 (2000) 49–51.
[26] Spatially addressed deposition and imaging of biochemically active bead microstructures by scanning electrochemical microscopy.
[27] C.A. Wijayawardhana, G. Wittstock, H.B. Halsall, W.R. Heineman, Anal. Chem. 72 (2000) 333–338.
[28] T. Wilhelm, G. Wittstock, Generation of periodic enzyme patterns by soft lithography and activity imaging by scanning electrochemical microscopy, Langmuir 18 (2002) 9485–9493.